

Received: 2020.01.02

Accepted: 2020.03.05

Available online: 2020.05.06

Published: 2020.06.28

# Down-Regulation of the Mammalian Target of Rapamycin (mTOR) Pathway Mediates the Effects of the Paeonol-Platinum(II) Complex in Human Thyroid Carcinoma Cells and Mouse SW1736 Tumor Xenografts

**Authors' Contribution:**

Study Design A  
Data Collection B  
Statistical Analysis C  
Data Interpretation D  
Manuscript Preparation E  
Literature Search F  
Funds Collection G

BCDE **Ling He\***  
BC **Song Guo\***  
BCD **Taiyang Zhu\***  
ADEF **Chen Chen**  
ABC **Kun Xu**

Department of General Surgery, Affiliated Hospital of Nanjing University of Chinese Medicine, Nanjing, Jiangsu, P.R. China

**Corresponding Authors:**  
**Source of support:**

\* Ling He, Song Guo and Taiyang Zhu are co-first authors, they contributed equally to this work  
Chen Chen, e-mail: chen1123chen@sina.com, Kun Xu, e-mail: edgarkun1976@sina.com  
Departmental sources

**Background:** This study aimed to investigate the effects of the paeonol-platinum(II) (PL-Pt[II]) complex on SW1736 human anaplastic thyroid carcinoma cell line and the BHP7-13 human thyroid papillary carcinoma cell line *in vitro* and on mouse SW1736 tumor xenografts *in vivo*.

**Material/Methods:** The cytotoxic effects of the PL-Pt(II) complex on SW1736 cells and BHP7-13 cells was measured using the MTT assay. Western blot measured the expression levels of cyclins, cell apoptotic proteins, and signaling proteins. DNA content and apoptosis were detected by flow cytometry. SW1736 cell thyroid tumor xenografts were established in mice followed by treatment with the PL-Pt(II) complex.

**Results:** Treatment of the SW1736 and BHP7-13 cells with the PL-Pt(II) complex reduced cell proliferation in a dose-dependent manner, with an IC50 of 1.25  $\mu$ M and 1.0  $\mu$ M, respectively, and increased the cell fraction in G0/G1 phase, inhibited p53, cyclin D1, promoted p27 and p21 expression, and significantly increased the sub-G1 fraction. Treatment with the PL-Pt(II) complex increased caspase-3 degradation, reduced the expression of p-4EBP1, p-4E-BP1 and p-S6, and reduced the expression of p-ERK1/2 and p-AKT. Treatment with the PL-Pt(II) complex reduced the volume of the SW1736 mouse tumor xenografts on day 14 and day 21, and reduced AKT phosphorylation and S6 protein expression and increased degradation of caspase-3.

**Conclusions:** The cytotoxic effects of the PL-Pt(II) complex in human thyroid carcinoma cells, including activation of apoptosis and an increased sub-G1 cell fraction of the cell cycle, were mediated by down-regulation of the mTOR pathway.

**MeSH Keywords:** **Apoptosis • Cyclin D1 • Thyroid Neoplasms**

**Full-text PDF:** <https://www.medscimonit.com/abstract/index/idArt/922561>

 2681

 —

 6

 46



## Background

Thyroid cancer originates from the follicular cells or parafollicular C cells in the thyroid gland and is a common endocrine malignancy [1]. Globally, the incidence of thyroid cancer has gradually increased over the past two decades because of the increasing diagnosis of cases of papillary carcinoma of the thyroid [2,3]. However, there has been no significant change in the incidence of follicular thyroid cancer [2,3]. The thyroid cancers also include anaplastic cancers and medullary thyroid cancers, and 5% of cases develop radioactive iodine-refractory tumors with an overall survival time of less than five years [4]. Anaplastic thyroid cancer is an aggressive malignancy that has an average overall survival of only six months [4]. Around 4% of patients with thyroid cancer have medullary thyroid cancer, for which the survival depends on the metastatic potential of the tumor [5,6]. There remains a need for novel and effective chemotherapy for the treatment of thyroid cancer.

The mammalian target of rapamycin (mTOR) signaling pathway plays a central role in the regulation of processes related to cell growth and is distributed in two different complexes, mTORC1 and mTORC2 [7–9]. The mTOR-related proteins include mLST8/GβL and PRAS40, which comprise mTORC1. The major effectors of mTORC1 are eIF4E-binding protein (4EBP1) along with the S6 kinase 1 [10]. In combination with mLST8/GβL, mSIN1, pTSC2, and rictor, mTOR includes mTORC2, which regulates the survival and proliferation of cells via AKT phosphorylation [11]. Abnormalities in the mTOR pathway are the common events detected in malignancy [7]. Cell growth regulation by mTOR involves the integration of signals obtained from various inputs [8]. The growth factors regulate mTOR through the involvement of the phosphatidylinositol-3-kinase (PI3K)/AKT pathway. However, growth factor-mediated regulation of mTOR is generally countered by phosphatase and tensin homolog (PTEN). During energy stress, AMP-activated protein kinase (AMPK) connects the energy status of the cells with mTORC1 [12]. Previous studies have demonstrated that overexpression of mTOR in cancers and phospho-mTOR is considered a marker of the aggressiveness of PTC [13,14].

The altered activity of cyclin-dependent kinases leads to proliferation of thyroid cancer cells, which is the characteristic of malignant tumors [15]. CDK4 and CDK6 induce the cellular transition to the G1 phase from G0 following activation from D-type cyclins. CDK2 drives the transition from G1 to the S phase while as complex comprised of CDK1-cyclin B1 catalyzes progression through M phase [16–18]. The activity of CDKs is altered in human cancer, and is associated with unrestricted cell proliferation [19,20]. Studies have shown that in medullary thyroid carcinoma, cell proliferative is increased by CDK5 expression [21,22]. CDK9 is involved in upregulation of RNA transcription via phosphorylation of RNA polymerase II

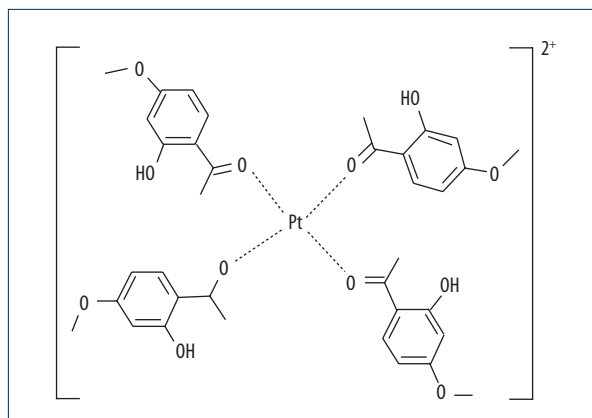


**Figure 1.** The structure of the paeonol-platinum(II) (PL-Pt(II)) complex.

at the C-terminal [23]. Therefore, control of CDK activity may inhibit tumor cell proliferation and has the potential to be a therapeutic target for thyroid cancer [24].

Metals that are complexed with platinum are commonly used chemotherapy agents, but they can have severe side effects. Copper metal complexes used as cancer therapeutic agents like cisplatin, oxaliplatin, and carboplatin have been found to induce various harmful effects despite possessing potential activity [25,26]. Platinum may undergo complex formation with organic compounds to eliminate side effects from chemotherapy, and the resulting complexes have shown efficient anticancer activity [25,27]. For example, early complexes of jatrorrhizine with platinum were reported to show potential anticancer activity [28–31].

Therefore, this study aimed to investigate the effects of the paeonol-platinum(II) (PL-Pt(II)) complex (Figure 1) on SW1736 human anaplastic thyroid carcinoma cell line and the BHP7-13 human thyroid papillary carcinoma cell line *in vitro* and on mouse SW1736 tumor xenografts *in vivo*.

## Material and Methods

### Cell lines

The SW1736 human anaplastic thyroid carcinoma cell line and the BHP7-13 human thyroid papillary carcinoma cell line were obtained from the cell bank of the Fourth Military Medical University, China. The cells were cultured in Dulbecco's modified Eagle's medium (DMEM) containing 10% fetal calf serum (FCS) (Gibco, Thermo Fisher Scientific, Waltham, MA, USA) in an incubator with a humidified atmosphere containing 5% CO<sub>2</sub> at 37°C. Penicillin (100,000 units/L) and streptomycin (100 mg/L) were added to the culture medium.

## MTT assay

The MTT assay measured the proliferation inhibitory activity of the paeonol-platinum(II) (PL-Pt(II)) complex for SW1736 and BHP7-13 cells. The cells were incubated with PL-Pt(II) at 0.25, 0.5, 0.75, 1.0, 1.25, 1.5, 1.75 and 2.0  $\mu\text{M}$  for 48 h. The MTT solution with a final concentration of 5 mg/ml was added to the plates, and the cells were incubated for 4 h. The MTT reduction produced water-insoluble blue formazan crystals. After the medium was removed, the cells were suspended in dimethyl sulfoxide (DMSO). The changes in absorbance by formazan produced were measured at 487 nm using a microplate reader (BioRad Labs, Hercules, CA, USA).

## Cell cycle assessment

The SW1736 and BHP7-13 cells incubated at  $1 \times 10^6$  cells per well in six-well plates were cultured in DMEM overnight. PL-Pt(II) at 1.0 and 2.0  $\mu\text{M}$  doses were mixed with medium, and the cells were incubated for 48 h. Trypsinization of the adherent cells was followed by washing in PBS and fixing with 70% ethyl alcohol. Then, RNase A and propidium iodide (PI) were added to the wells and incubated for 20 min. The DNA content of cells was detected using flow cytometry using a BD FACSCalibur flow cytometer (BD Biosciences, Franklin Lakes, NJ, USA) to assess the cell cycle.

## Annexin V/propidium iodide (PI) assay

The apoptotic cell count in SW1736 and BHP7-13 cells was measured using an apoptosis detection kit (Immunotech Co., Marseille, France). The cells distributed at  $1 \times 10^6$  cells per dish in 60 mm culture plates were treated with PL-Pt(II) at 1.0 and 2.0  $\mu\text{M}$  for 48 h. Then cells were rinsed twice in cold-PBS followed by incubation for 20 min with AnnexinV and PI. The count of the apoptotic cells was determined by flow cytometry using Modfit software (Verity Software House, Inc., Topsham, ME, USA).

## Western blot

The SW1736 and BHP7-13 cells were incubated at  $2 \times 10^5$  cells per well in 100 mm Petri dishes in DMEM medium and cultured overnight. PL-Pt(II) at 1.0 and 2.0  $\mu\text{M}$  was added to the plates, and cell incubation was performed for 48 h. The dissolution of cell pellets was performed in radio-immunoprecipitation (RIPA) buffer and a protease inhibitor cocktail for 25 min at 4°C. The samples were centrifuged at  $13,000 \times g$  for 30 min, and the protein concentration was assessed by using a BCA kit (Pierce, Rockford, IL, USA). The protein lysate in equal quantities was separated on a 12% sodium dodecyl sulfate-polyacrylamide gel electrophoresis (SDS-PAGE) gel and subsequently electroblotted onto nitrocellulose membranes (Merck Millipore, Burlington, MA, USA). The membranes were incubated with TBS

mixed with Tween-20 (0.1%) with 5% dried skimmed milk powder at room temperature for 3 h. The proteins were probed by incubation with primary antibodies overnight at 4°C. The primary antibodies used were to p-AKT, AKT, p-4E-BP1, 4E-BP1, p-S6, S6, p-ERK1/2, ERK1/2, p21, p27, cyclin D1 and caspase-3 (Cell Signaling Technology, Danvers, MA, USA). After washing with PBS, the membranes were incubated for 2 h with horseradish peroxidase (HRP)-conjugated anti-rabbit IgG secondary antibodies. The enhanced chemiluminescence kit (Bionovas Biotechnology Co., Ltd., Toronto, ON, Canada) in combination with the Molecular Imager VersaDoc MP 4000 system (Bio-Rad, Hercules, CA, USA) were used to detect the protein bands.

## The SW1736 cell mouse xenografts

Thirty 6-week-old female athymic mice, weighing 26–30 gm, were obtained from the Shanghai SLAC Laboratory Animal Company, China. The mice were housed at  $23 \pm 2^\circ\text{C}$  under pathogen-free conditions in an animal center in 70% relative humidity with a 12-hourly light and dark cycle. All animal experiments were performed according to The International Guidelines for the Care and Treatment of Animals. This study was approved by the Animal Ethics Committee, Nanjing University of Chinese Medicine (Approval No: 2008112401). The mouse studies were conducted in accordance with the guidelines issued by the National Institutes of Health, China.

The mice were randomly assigned to three groups, the sham group, the vehicle-control group, and the PL-Pt(II) treatment group. The SW1736 cells ( $1 \times 10^8$ ) in 0.3 mL of normal saline were subcutaneously inoculated into the right flank. The mice were treated with 2 mg/kg of PL-Pt(II) or vehicle through an intra-gastric route for 21 days, daily, until day 28. The mice in the vehicle control group were injected with 200  $\mu\text{L}$  of normal saline. The tumor volumes were measured in each mouse with a slide caliper till day 28. The body weight was also measured as a marker of toxicity.

## Determination of p-AKT, p-S6, PCNA and caspase-3 in tumors

The mice were euthanized on day 29 of the treatment, using carbon dioxide inhalation, and the xenograft tumors were removed. The excised tumors were treated with protein extraction buffer (GE Healthcare Life Sciences, Logan, UT, USA) followed by homogenization and sonicated at a cool temperature. The samples were centrifuged, and the supernatants were stored under liquid nitrogen for Western blot.

## Statistical analysis

Data were analyzed using one-way analysis of variance (ANOVA) and Bonferroni's multiple comparison test. Data were presented as the mean  $\pm$  standard deviation (SD) of three experiments.

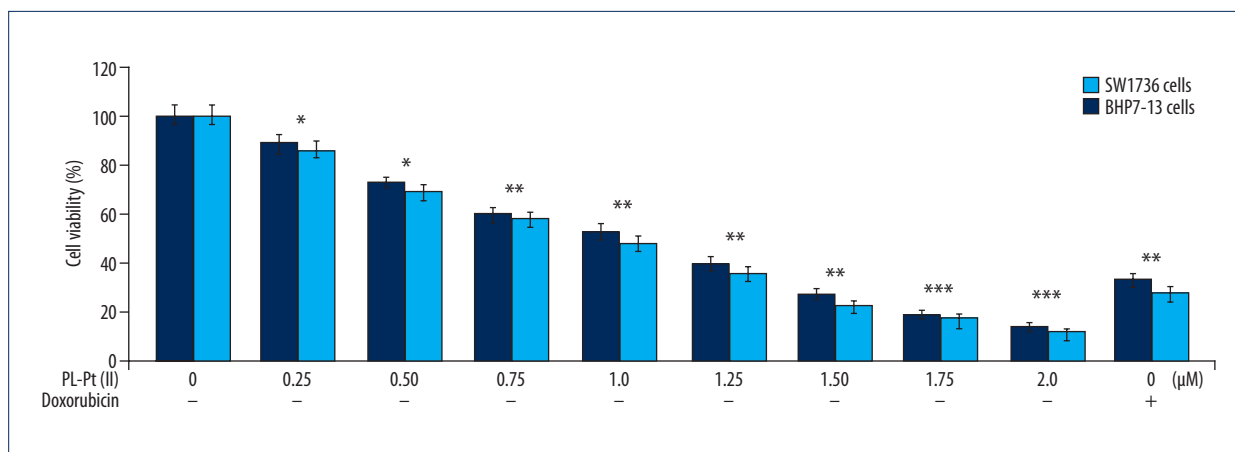


**Figure 2.** The effect of the paeonol-platinum(II) (PL-Pt(II)) complex on the viability of SW1736 human anaplastic thyroid carcinoma cells and BHP7-13 human thyroid papillary carcinoma cells. The changes in SW1736 and BHP7-13 cell growth was measured at the indicated concentrations of PL-Pt(II) using the MTT assay. \*  $P < 0.05$ ; \*\*  $P < 0.02$  and \*\*\*  $P < 0.01$  vs. untreated cells.

Analysis was performed using SPSS version 17.0 software (SPSS, Inc., Chicago, IL, USA).  $P > 0.05$  represented a statistically significant difference.

## Results

### Cytotoxicity of the paeonol-platinum(II) (PL-Pt(II)) complex in SW1736 and BHP7-13 cells

PL-Pt(II) treatment reduced cell proliferation of SW1736 and BHP7-13 cells in a dose-dependent manner (Figure 2). The changes in cell proliferation associated with doses of 0.25, 0.5, 0.75, 1.0, 1.25, 1.5, 1.75, and 2.0  $\mu\text{M}$  of PL-Pt(II) were measured at 48 h by the MTT assay. The SW1736 and BHP7-13 cell growth were reduced by 40% at 0.75  $\mu\text{M}$  PL-Pt(II). At 2  $\mu\text{M}$  of PL-Pt(II) cell growth was reduced by 85% in SW1736 and BHP7-13 cells at 48 h. The IC<sub>50</sub> of PL-Pt(II) for SW1736 and BHP7-13 cells was 1.25 and 1.0  $\mu\text{M}$ , respectively, following treatment for 48 h. Doxorubicin at 0.16  $\mu\text{M}$  reduced SW1736 and BHP7-13 cell proliferation to 33% and 28%, respectively.

### The effects of PL-Pt(II) on the SW1736 and BHP7-13 cell cycle

The SW1736 and BHP7-13 cells at 48 h of PL-Pt(II) treatment at 1.0 and 2.0  $\mu\text{M}$  were assessed for DNA content and distribution (Figure 3A–3D). PL-Pt(II) treatment of SW1736 and BHP7-13 cells increased the cell fraction in the G<sub>0</sub>/G<sub>1</sub> phase. The SW1736 and BHP7-13 cell fraction in the S phase and G<sub>2</sub>/M phase were reduced following treatment with 1.0 and 2.0  $\mu\text{M}$  PL-Pt(II). The PL-Pt(II)-induced changes in G<sub>0</sub>/G<sub>1</sub> linked proteins were also assessed in SW1736 and BHP7-13 cells treated with 1.0 and 2.0  $\mu\text{M}$  of PL-Pt(II) (Figure 3E). In SW1736 and BHP7-13 cells, p53 and cyclin D1 expression were reduced,

while p27 and p21 expression were upregulated following treatment with 1.0 and 2.0  $\mu\text{M}$  of PL-Pt(II).

### The effects of PL-Pt(II) on SW1736 and BHP7-13 cell apoptosis

Apoptosis activation by 1.0 and 2.0  $\mu\text{M}$  PL-Pt(II) in SW1736 and BHP7-13 cells was also explored at 48 h (Figure 4A, 4B). Compared with the untreated controls, PL-Pt(II) at 1.0 and 2.0  $\mu\text{M}$  significantly promoted apoptosis induction, which was evident from sub-G<sub>1</sub> cell fraction. The sub-G<sub>1</sub> fraction of cells increased significantly in SW1736 and BHP7-13 cells on treatment with 1.0 and 2.0  $\mu\text{M}$  PL-Pt(II). The PL-Pt(II) induced apoptosis in SW1736 and BHP7-13 cells were also validated by the assessment of caspase-3 degradation (Figure 4C). In PL-Pt(II) treated cells, caspase-3 degradation was detected markedly compared with the untreated controls.

### PL-Pt(II) modulated the mTOR pathways in SW1736 and BHP7-13 cells

The PL-Pt(II) induced changes in p-4EBP1, 4E-BP1, and p-S6 proteins in SW1736 and BHP7-13 cells was assessed using Western blot (Figure 5). Treatment with 1.0 and 2.0  $\mu\text{M}$  PL-Pt(II) significantly down-regulated the expression of p-4EBP1, p-4E-BP1, and p-S6 in SW1736 and BHP7-13 cells. In SW1736 and BHP7-13 cells, treatment with 1.0 and 2.0  $\mu\text{M}$  PL-Pt(II) down-regulated the expression of p-ERK1/2 and p-AKT. These findings indicated that PL-Pt(II) had an inhibitory effect on the mTOR pathway in SW1736 and BHP7-13 cells.

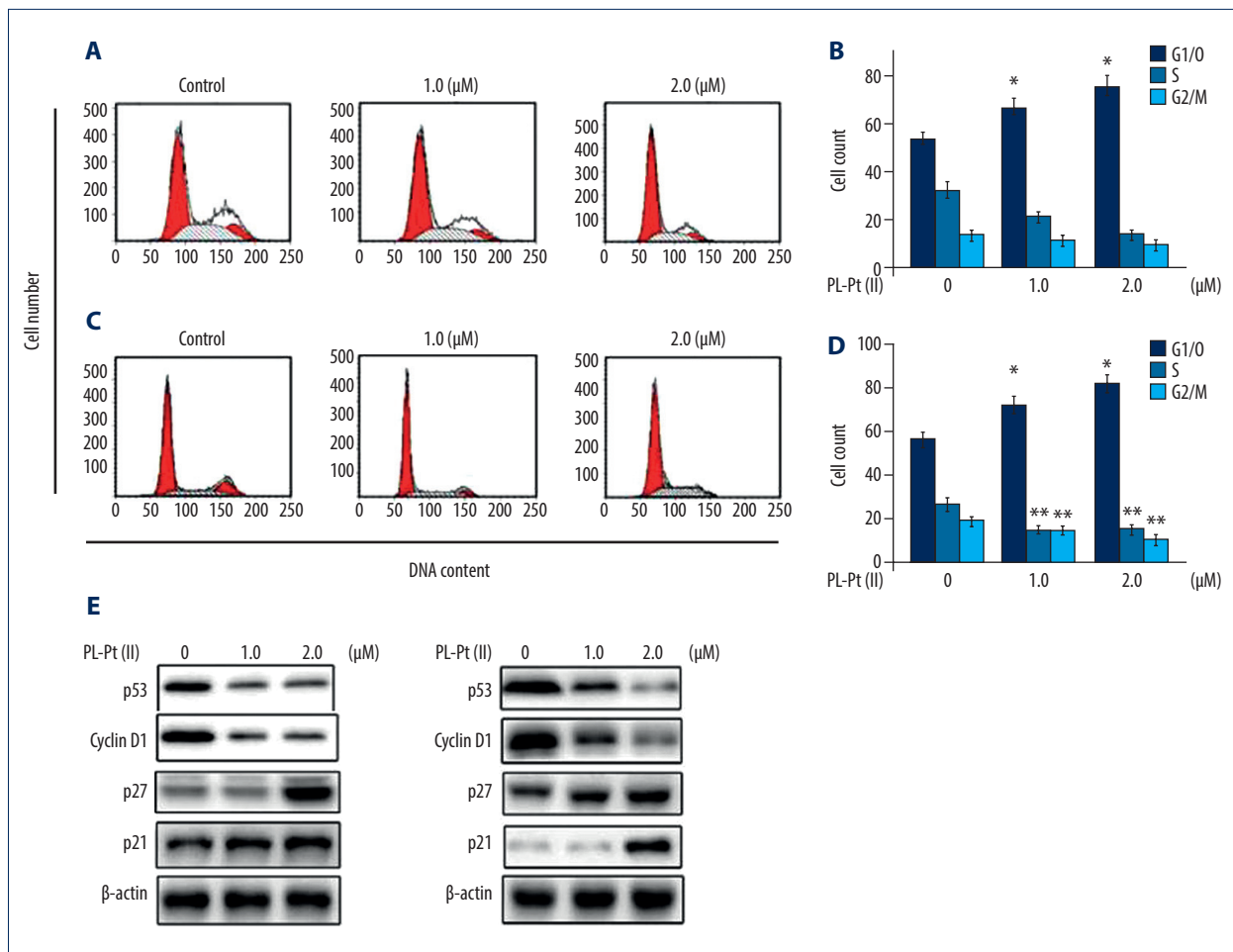


**Figure 3.** The inhibitory effect of the paeonol-platinum(II) (PL-Pt[II]) complex on the cell cycle in SW1736 human anaplastic thyroid carcinoma cells and BHP7-13 human thyroid papillary carcinoma cells. **(A–D)** The DNA content in PL-Pt(II)-treated SW1736 cells and BHP7-13 cells, detected by flow cytometry using propidium iodide (PI) staining. **(E)** The proteins regulating the cell cycle were assessed using Western blot in SW1736 and BHP7-13 cells treated with 1.0 and 2.0 μM of PL-Pt(II). \*  $P < 0.05$  and \*\*  $P < 0.01$  vs. untreated cells.

### The effect of PL-Pt(II) on mouse SW1736 cell tumor xenografts

The athymic nude mice developed SW1736 cell subcutaneous xenografts in the flank. The mice with established xenografts were treated with 2 mg/kg of PL-Pt(II) or vehicle for 21 days daily and until day 28 (Figure 6A). The tumor volume showed a statistically significant difference between the PL-Pt(II) treated and vehicle-treated control mice on day 14 ( $73.1 \pm 18.5 \text{ mm}^3$  and  $298.1 \pm 45.7 \text{ mm}^3$ ;  $P = 0.01$ ) and day 21 ( $92.3 \pm 21.8 \text{ mm}^3$  and  $465.7 \pm 82.3 \text{ mm}^3$ ;  $P = 0.02$ ). However, there was a difference in tumor volume between PL-Pt(II) treated and vehicle-treated control mice ( $465.7 \pm 88.5 \text{ mm}^3$  and  $802.6 \pm 130.5 \text{ mm}^3$ ;  $P = 0.18$ ) decreased on day 28, or day 8 of treatment discontinuation. The bodyweight of PL-Pt(II)-treated and the vehicle-treated control mice did not show a significant difference during the study (Figure 6B). In PL-Pt(II)-treated mice,

AKT phosphorylation, and S6 protein expression were significantly down-regulated (Figure 6C). Also, caspase-3 degradation was increased in mice treated with PL-Pt(II).

### Discussion

The findings from the present study showed that the paeonol-platinum(II) (PL-Pt[II]) complex effectively suppressed the proliferation of SW1736 and BHP7-13 thyroid cancer cells *in vitro*. The activity of PI3K/mTOR pathway is higher in the carcinoma cells bearing PTEN deletion or mutated PI3K gain-of-function [32]. The aggressiveness of thyroid cancer depends on PI3K/mTOR activation, and targeting this pathway impairs thyroid cancer growth [32]. It has been reported that mTORC1 inhibition by therapeutic agents in low doses causes S6 kinase 1 inactivation followed by mTORC2 activation, which increased p-AKT by

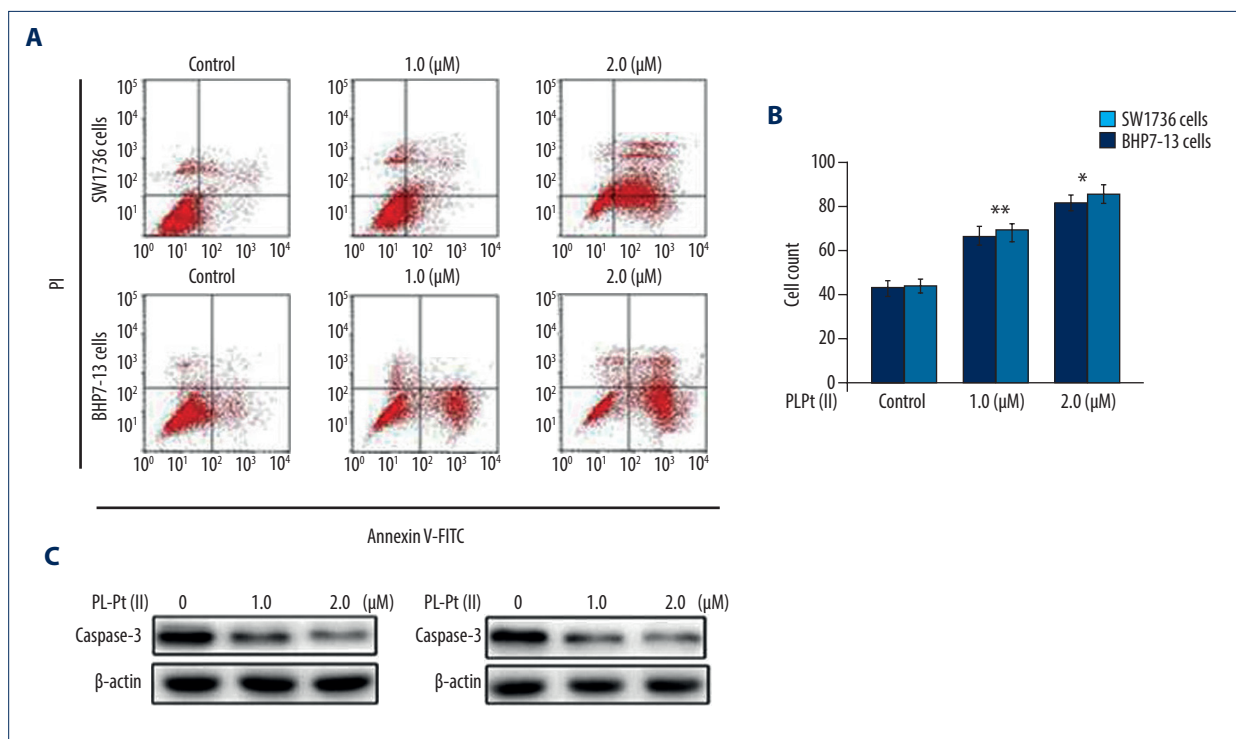


**Figure 4.** The apoptotic effects of the paeonol-platinum(II) (PL-Pt(II)) complex on SW1736 human anaplastic thyroid carcinoma cells and BHP7-13 human thyroid papillary carcinoma cells. **(A, B)** The fraction of sub-G1 cells measured using flow cytometry at 48 h of treatment with 1.0 and 2.0 μM of PL-Pt(II). **(C)** Caspase-3 degradation in SW1736 and BHP7-13 cells treated with 1.0 and 2.0 μM of PL-Pt(II) assessed by Western blot. \* P<0.05 and \*\* P<0.01 vs. untreated cells.

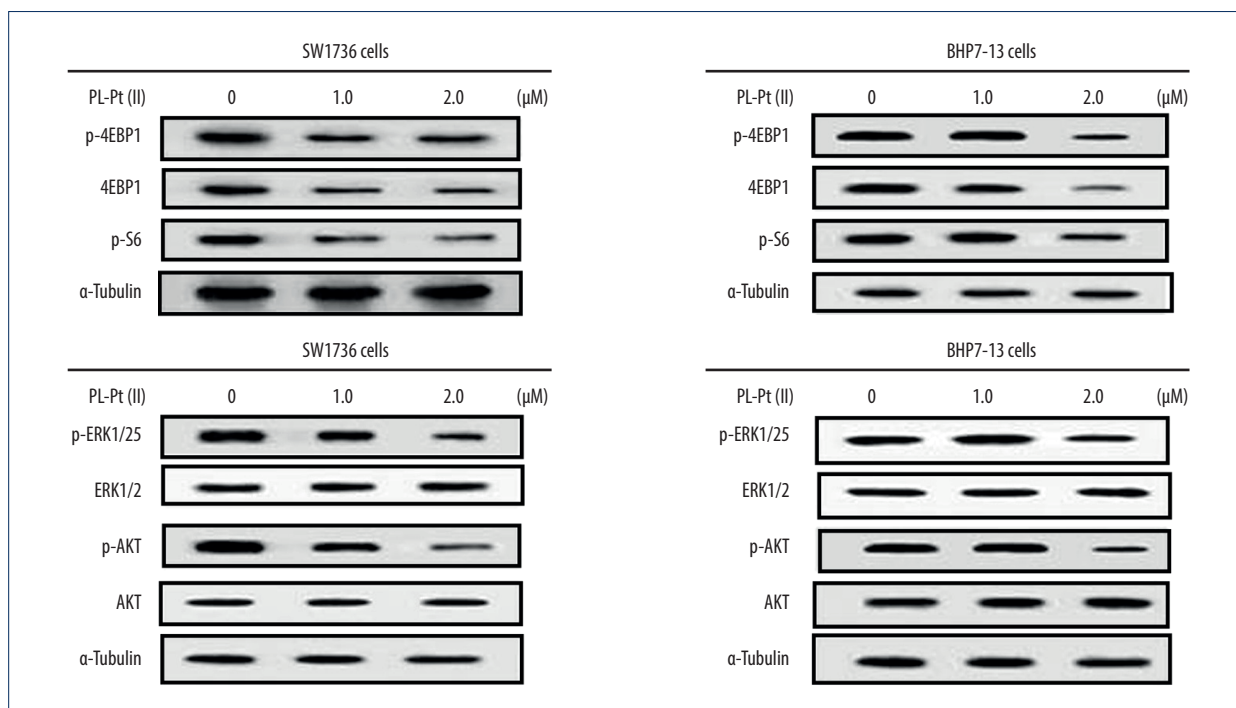


**Figure 5.** The effects of the paeonol-platinum(II) (PL-Pt(II)) complex on the mTOR pathway in SW1736 human anaplastic thyroid carcinoma cells and BHP7-13 human thyroid papillary carcinoma cells. The expression of p-ERK1/2, p-AKT, p-4EBP1, p-4E-BP1, and p-S6 in SW1736 and BHP7-13 cells after treatment with 1.0 and 2.0 μM of PL-Pt(II) was assessed by Western blot.

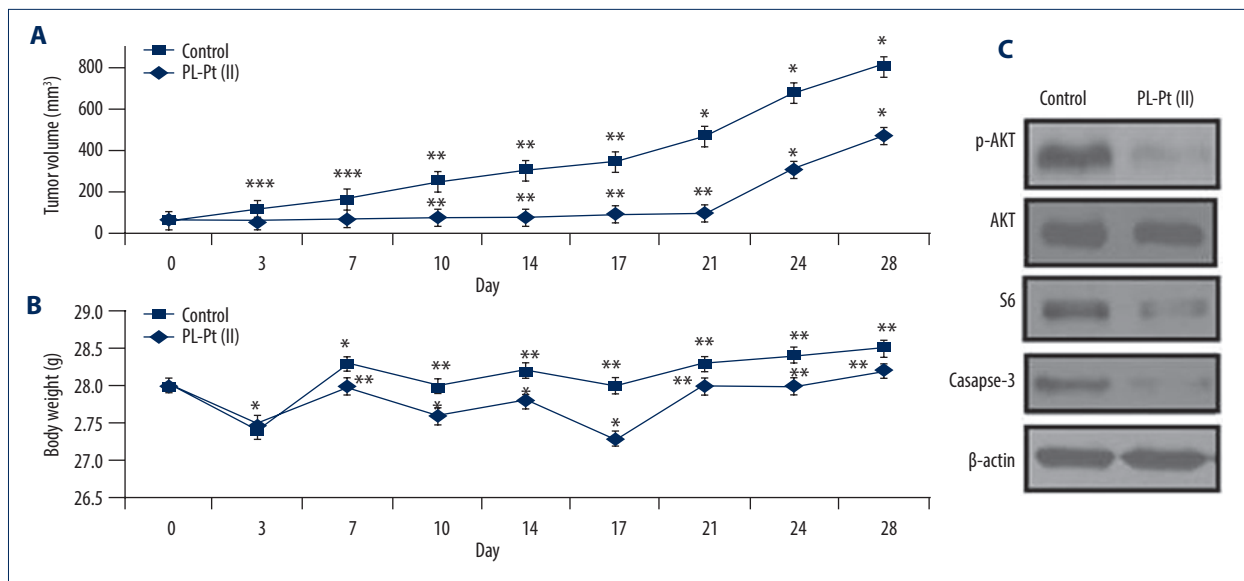


**Figure 6.** The inhibitory effect of the paeonol-platinum(II) (PL-Pt[II]) complex on mouse SW1736 cell tumor xenografts *in vivo*. (A) PL-Pt(II) (2 mg/kg) gavage was given daily for 21 days to the mice bearing the SW1736 cell xenografts, which reduced tumor volume. (B) The toxicity of PL-Pt(II) *in vivo* was evaluated by measuring body weight during the study. (C) The effect of PL-Pt(II) on p-AKT, p-S6, caspase-3, and p-S6 in the mouse tumor xenografts were detected by Western blot. \* P<0.05, \*\* P<0.02 and \*\*\* P<0.01 vs. Day 0.

a negative loop mechanism [33]. However, mTORC2 activation and p-AKT enhancement was overcome by the use of higher dose therapeutic agents [34,35]. In the present study, PL-Pt(II) inhibited SW1736 and BHP7-13 cell proliferative potential via apoptosis induction. The caspase-3 degradation in SW1736 and BHP7-13 cells by PL-Pt(II) treatment markedly elevated. Studies have demonstrated elevated levels of inhibitors of cyclin-dependent kinases, p21, and p27 associated with the apoptosis activation and arrest of the cell cycle in different cancer cells [36–38]. The universal inhibitors of CDKs, p21, and p27 directly target cyclin-CDK complexes activities in the cells [39,40].

The cell fraction in the G1/G0 phase was also increased by PL-Pt(II) in SW1736 and BHP7-13 cell. The arrest of the SW1736 and BHP7-13 cell cycle by PL-Pt(II) was supported by the inhibition of p53 and cyclin D1 expression. However, p27 and p21 expressions were increased in PL-Pt(II)-treated cells. PL-Pt(II) inhibited phosphorylation of PI3K and mTOR in SW1736 and BHP7-13 cells. These findings supported the anti-proliferative activity of PL-Pt(II) for thyroid cancer cells by targeting the PI3K/mTOR pathway. The activation of mTORC1 induces expression of S6 ribosomal protein, which is a downstream component of the S6 kinase 1 [41–43]. The p-S6 protein phosphorylation promotes the translation of proteins that increase the growth of cells.

The efficiency of mTOR inhibitors as therapeutic agents for sarcoma has been shown by p-S6 protein expression [44]. A previous study showed an inverse association between PI3K/mTOR activation and p27 expression, and targeting this pathway promoted

the expression of p27 [45]. The down-regulation of mTORC1 dephosphorylates 4E-BP1, followed by its binding to eIF4E, which blocks protein translation and cell proliferation [42,43]. The findings from the present study showed upregulation of p27 and down-regulation of p-S6 in SW1736 and BHP7-13 cells treated with PL-Pt(II). PL-Pt(II) treatment also inhibited p-4EBP1 and p-4E-BP1 protein expression in SW1736 and BHP7-13 cells. Also, mTORC1 plays an important role in regulating the cell cycle and cell apoptosis in different cells [43]. The inhibitory effect of PL-Pt(II) also included the down-regulation of mTORC1 in SW1736 and BHP7-13 cells. In the present study PL-Pt(II) treatment suppressed *in vivo* tumor xenograft growth in the mice without inducing toxicity. However, tumor growth inhibition by PL-Pt(II) was not effective after treatment discontinuation probably because mTOR, S6 Kinase 1, and 4E-BP1 were re-activated [46]. Degradation of caspase-3 and reduced expression of PCNA were promoted *in vivo* by treatment with PL-Pt(II).

## Conclusions

This study aimed to investigate the effects of the paeonol-platinum(II) (PL-Pt[II]) complex on SW1736 human anaplastic thyroid carcinoma cell line and the BHP7-13 human thyroid papillary carcinoma cell line *in vitro* and on mouse SW1736 tumor xenografts *in vivo*. The PL-Pt(II) complex induced cytotoxicity for thyroid cancer cells by down-regulating the mTOR pathway, activated cell apoptosis, and increased the sub-G1 cell fraction in SW1736 and BHP7-13 cells.

## References:

- Lin S-F, Huang Y-Y, Lin J-D et al: Utility of a PI3K/mTOR inhibitor (NVP-BEZ235) for thyroid cancer therapy. *PLoS One*, 2012; 7(10): e46726
- Davies L, Welch HG: Increasing incidence of thyroid cancer in the United States, 1973–2002. *JAMA*, 2006; 295: 2164–67
- Chen AY, Jemal A, Ward EM: Increasing incidence of differentiated thyroid cancer in the United States, 1988–2005. *Cancer*, 2009; 115: 3801–7
- Ricarte-Filho JC, Ryder M, Chitale DA et al: Mutational profile of advanced primary and metastatic radioiodine-refractory thyroid cancers reveals distinct pathogenetic roles for BRAF, PIK3CA, and AKT1. *Cancer Res*, 2009; 69: 4885–93
- Nikiforov YE, Nikiforova MN: Molecular genetics and diagnosis of thyroid cancer. *Nat Rev Endocrinol*, 2011; 7: 569–80
- Sjppel RS, Kunimallaiyaan M, Chen H: Current management of medullary thyroid cancer. *Oncologist*, 2008; 13: 539–47
- Faustino A, Couto JP, Pópulo H et al: mTOR pathway overactivation in BRAF mutated papillary thyroid carcinoma. *J Clin Endocrinol Metab*, 2012; 97: E1139–49
- Miyakawa M, Tsumihima T, Murakami H et al: Increased expression of phosphorylated p70S6 and Akt in papillary thyroid cancer tissues. *Endocr J*, 2003; 50: 77–83
- Wulschleger S, Loewith R, Hall MN: TOR signaling in growth and metabolism. *Cell*, 2006; 124: 471–84
- Hay N, Sonenberg N: Upstream and downstream of mTOR. *Genes Dev*, 2004; 18: 1926–45
- Sarbasov DD, Guertin DA, Ali SM, Sabatini DM: Phosphorylation and regulation of Akt/PKB by the rictor-mTOR complex. *Science*, 2005; 307: 1098–101
- Guertin DA, Sabatini DM: An expanding role for mTOR in cancer. *Trends Mol Med*, 2005; 11: 353–61
- Hardie DG, Scott JW, Pan DA, Hudson ER: Management of cellular energy by the AMP-activated protein kinase system. *FEBS Lett*, 2003; 546: 113–20
- Tavares C, Eloy C, Melo M et al: mTOR pathway in papillary thyroid carcinoma: Different contributions of mTORC1 and mTORC2 complexes for tumor behavior and SLC5A5 mRNA expression. *Int J Mol Sci*, 2018; 19(5): pii: E1448
- Lin S-F, Lin J-D, Hsueh C, Chou T-C, Wong RJ: A cyclin-dependent kinase inhibitor, dinaciclib in preclinical treatment models of thyroid cancer. *PLoS One*, 2017; 12(2): e0172315
- Malumbres M, Barbacid M: To cycle or not to cycle: A critical decision in cancer. *Nat Rev Cancer*, 2001; 1(3): 222–31
- Malumbres M, Barbacid M: Cell cycle, CDKs and cancer: A changing paradigm. *Nat Rev Cancer*, 2009; 9: 153–66
- Merrick KA, Fisher RP: Why minimal is not optimal: driving the mammalian cell cycle and drug discovery with a physiologic CDK control network. *Cell Cycle*, 2012; 11: 2600–5
- Ortega S, Malumbres M, Barbacid M: Cyclin D-dependent kinases, INK4 inhibitors and cancer. *Biochim Biophys Acta*, 2002; 1602: 73–87
- Malumbres M: Physiological relevance of cell cycle kinases. *Physiol Rev*, 2011; 91: 973–1007
- Kawauchi T: Cdk5 regulates multiple cellular events in neural development, function and disease. *Dev Growth Differ*, 2014; 56: 335–48
- Pozo K, Castro-Rivera E, Tan C et al: The role of Cdk5 in neuroendocrine thyroid cancer. *Cancer Cell*, 2013; 24: 499–511
- Bywater MJ, Pearson RB, McArthur GA, Hannan RD: Dysregulation of the basal RNA polymerase transcription apparatus in cancer. *Nat Rev Cancer*, 2013; 13: 299–314
- Asghar U, Witkiewicz AK, Turner NC, Knudsen ES: The history and future of targeting cyclin-dependent kinases in cancer therapy. *Nat Rev Drug Discov*, 2015; 14: 130–46
- Frik M, Fernández-Gallardo J, Gonzalo O et al: Cyclometalated imino-phosphorane gold(III) and platinum(II) complexes. A highly permeable cationic platinum(II) compound with promising anticancer properties. *J Med Chem*, 2015; 58: 5825–41
- Medici S, Peana M, Nurchi VM et al: Noble metals in medicine: Latest advances. *Coord Chem Rev*, 2015; 284: 329–50
- Monroe JD, Hruska HL, Ruggles HK et al: Anti-cancer characteristics and ototoxicity of platinum(II) amine complexes with only one leaving ligand. *PLoS One*, 2018; 13: e0192505
- Chen ZF, Qin QP, Qin JL et al: Water-soluble ruthenium(II) complexes with chiral 4-(2, 3-dihydroxypropyl)-formamide oxoaporphine (FOA): *In vitro* and *in vivo* anticancer activity by stabilization of G-Quadruplex DNA, inhibition of telomerase activity, and induction of tumor cell apoptosis. *J Med Chem*, 2015; 58: 4771–89
- Qin QP, Wang ZF, Huang XL et al: High *in vitro* and *in vivo* tumor-selective novel ruthenium(II) complexes with 3-(2'-Benzimidazolyl)-7-fluoro-coumarin. *ACS Med Chem Lett*, 2019; 10: 936–40
- Wang Y, Pang W, Zeng Q et al: Synthesis and biological evaluation of new berberine derivatives as cancer immunotherapy agents through targeting IDO1. *Eur J Med Chem*, 2018; 143: 1858–68
- Li J, Li J, Jiao Y, Dong C: Spectroscopic analysis and molecular modeling on the interaction of jatrorrhizine with human serum albumin (HSA). *Spectrochim Acta A Mol Biomol Spectrosc*, 2014; 118: 48–54
- Santiskulvong C, Konecny GE, Fekete M et al: Dual targeting of phosphoinositide 3-kinase and mammalian target of rapamycin using NVP-BEZ235 as a novel therapeutic approach in human ovarian carcinoma. *Clin Cancer Res*, 2011; 17: 2373–84
- Foster KG, Fingar DC: Mammalian target of rapamycin (mTOR): Conducting the cellular signaling symphony. *J Biol Chem*, 2010; 285: 14071–77
- Serra V, Markman B, Scaltriti M et al: NVPBEZ235, a dual PI3K/mTOR inhibitor, prevents PI3K signaling and inhibits the growth of cancer cells with activating PI3K mutations. *Cancer Res*, 2008; 68: 8022–30
- Manara MC, Nicoletti G, Zambelli D et al: NVP-BEZ235 as a new therapeutic option for sarcomas. *Clin Cancer Res*, 2010; 16: 530–40
- Engelman JA: Targeting PI3K signalling in cancer: Opportunities, challenges and limitations. *Nat Rev Cancer*, 2009; 9: 550–62
- Faivre S, Kroemer G, Raymond E: Current development of mTOR inhibitors as anticancer agents. *Nat Rev Drug Discov*, 2006; 5: 671–88
- Hennessy BT, Smith DL, Ram PT et al: Exploiting the PI3K/AKT pathway for cancer drug discovery. *Nat Rev Drug Discov*, 2005; 4: 988–1004
- Wang XY, Penalba LO, Yuan H et al: Musashi1 regulates breast tumor cell proliferation and is a prognostic indicator of poor survival. *Mol Cancer*, 2010; 9: 221
- Wang YF, Chen NS, Chung YP et al: Sodium butyrate induces apoptosis and cell cycle arrest in primary effusion lymphoma cells independently of oxidative stress and p21 CIP1/WAF1 induction. *Mol Cell Biochem*, 2006; 285: 51–59
- Møller MB: p27 in cell cycle control and cancer. *Leuk Lymphoma*, 2000; 39: 19–27
- Liu DF, Ferguson K, Cooper GS et al: p27 cell-cycle inhibitor is inversely correlated with lymph node metastases in right-sided colon cancer. *J Clin Lab Anal*, 1999; 13: 291–95
- Coqueret O: New roles for p21 and p27 cell-cycle inhibitors: A function for each cell compartment? *Trends Cell Biol*, 2003; 13(2): 65–70
- Iwenofu OH, Lackman RD, Staddon AP et al: Phospho-S6 ribosomal protein: A potential new predictive sarcoma marker for targeted mTOR therapy. *Mod Pathol*, 2008; 21: 231–37
- Motti ML, Califano D, Troncione G et al: Complex regulation of the cyclin-dependent kinase inhibitor p27kip1 in thyroid cancer cells by the PI3K/AKT pathway: Regulation of p27kip1 expression and localization. *Am J Pathol*, 2005; 166: 737–49
- Fingar DC, Salama S, Tsou C et al: Mammalian cell size is controlled by mTOR and its downstream targets S6K1 and 4EBP1/eIF4E. *Genes Dev*, 2002; 16: 1472–87